Available on CMS information server

CMS CR -2012/289

The Compact Muon Solenoid Experiment

Conference Report

Mailing address: CMS CERN, CH-1211 GENEVA 23, Switzerland

30 October 2012 (v3, 31 October 2012)

Quarkonia production in heavy ion collisions at TeV energies

Michael Murray for the CMS Collaboration

Abstract

The CMS experiment at the LHC has measured the production of several quarkonium S states in both PbPb and pp collisions at a center-of-mass energy per nucleon pair of 2.76 TeV. The various states are measured from the dimuon invariant mass spectra. The yields of quarkonia in PbPb collisions are lower than expected from the corresponding pp yields scaled by the number of nucleon-nucleon collisions. This suppression is stronger for more central collisions. For the J/ψ at high p_T the suppression is stronger than that observed at lower energies and high p_T and stronger than at more forward rapidities and low p_T. The suppression is weakest for the $\Upsilon(1S)$ but increases as one moves to the J/ψ, $\psi(2S)$ the $\Upsilon(2S)$ and finally the $\Upsilon(3S)$.

Presented at *BEACH 2012: 10th International Conference On Hyperons, Charm And Beauty Hadrons*

Available online at www.sciencedirect.com
ScienceDirect
Nuclear Physics B Proceedings Supplement 00 (2012) 1–3
Nuclear Physics B Proceedings Supplement

Quarkonia production in heavy-ion collisions at TeV energies

Michael Murray for the CMS collaboration
University of Kansas

Abstract

The CMS experiment at the LHC has measured the production of several quarkonium S states in both PbPb and pp collisions at a center-of-mass energy per nucleon pair of 2.76 TeV. The various states are measured from the dimuon invariant mass spectra. The yields of quarkonia in PbPb collisions are lower than expected from the corresponding pp yields scaled by the number of nucleon-nucleon collision. For $\Upsilon(1S)$ and $\Upsilon(2S)$ and high p_T J/ψ this suppression is stronger for more central collisions. For the J/ψ at high p_T the suppression is stronger than that observed at lower energies and high p_T and stronger than at more forward rapidities and low p_T. The suppression is weakest for the $\Upsilon(1S)$ but increases as one moves to the J/ψ, $\psi(2S)$ the $\Upsilon(2S)$ and finally the $\Upsilon(3S)$.

Keywords:
Quarkonia, Heavy Ions

1. Introduction

In 1986 Matsui & Satz proposed that Debye screening in a Quark Gluon Plasma, (QGP), could lead to the melting of quarkonia [1]. Different binding energy of various bound states would then naturally lead to sequential melting of the states with increasing temperature. Recently Mocsy has calculated how the sequential melting of the various quarkonia states could serve as a thermometer of heavy ion collisions [2]. States with large radii should be susceptible to Debye screening at lower temperatures than more tightly bound states with small radii. Table 1 summarizes the properties of the first 5 quarkonia S wave states. The simple model of sequential melting described above is complicated by feed-down between states. The suppression of the $c\bar{c}$ and $b\bar{b}$ excited states may affect the observed yields of the ground states because of a reduction in the feed-down effect.

Since quarkonia are bound states of heavy $q-\bar{q}$ pairs, they can be studied with non-relativistic QCD. This provides an opportunity to have a very well understood system in pp collisions. Elsewhere in these proceedings Yu Zheng has summarized CMS pp measurements of the $J/\psi, \psi(2S)$ and $\Upsilon(nS)$ states, as a function of transverse momentum, p_T and rapidity [3]. There is good agreement between the measured cross sections and theory calculations, for the five S-wave quarkonia states. This paper will concentrate on the use of the quarkonia states to search for a quark gluon plasma.

Table 1: Masses in GeV/c^2 and characteristic radii in fermi for the first 5 quarkonia S states.

State	J/ψ	$\psi(2S)$	$\Upsilon(1S)$	$\Upsilon(2S)$	$\Upsilon(3S)$
Mass	3.10	3.68	9.46	10.02	10.36
Radius	0.50	0.90	0.28	0.56	0.78

2. The CMS experiment and analysis method

The central feature of CMS is a superconducting solenoid of 6m internal diameter, providing a magnetic field of 3.8T. Within the field volume are the silicon pixel and strip tracker, the crystal electromagnetic calorimeter, and the brass/scintillator hadron calorimeter. The silicon pixel and strip tracker measures charged-particle trajectories in the range $|\eta| < 2.5$. The tracker consists of 66 million pixel and 10 million strip sensor elements. Muons are detected in the range $|\eta| < 2.4$, with detection planes based on three technologies: drift tubes, cathode strip chambers, and resistive plate chambers. Because of the strong magnetic field and the fine granularity of the tracker, the muon p_T resolution is between 1 and 2% for a typical muon in this analysis. For more details on the detector see [4]. The PbPb and pp datasets used in the analysis correspond to integrated luminosities of 150 μb^{-1} and 230 nb^{-1} respectively, collected in 2011. All data presented in this paper are available at [5, 6, 7].

The forward region, $2.9 < |\eta| < 5.2$, is covered by two steel/quartz-fiber Čerenkov calorimeters (HF) which are used for event selection and centrality determination in PbPb collisions. In order to eliminate contamination from cosmic rays and ultra-peripheral electromagnetic events all PbPb events are required to have at least two tracks and more than 3 GeV deposited in at least 3 towers of HF.

The event centrality observable corresponds to the fraction of the total inelastic cross section, starting at 0% for the most central collisions and evaluated as percentiles of the distribution of the energy deposited in the HF [8, 9]. Using a Glauber-model calculation as described in Ref. [8], the average number of nucleons participating in the collisions (N_{part}) and the average nuclear overlap function T_{AA} have been estimated for each centrality class. T_{AA} is the ratio of the number of elementary nucleon-nucleon binary collisions to the nucleon-nucleon cross section and serves as an effective nucleon-nucleon luminosity [10]. In order to compare the number of quarkonia produced in PbPb, N_{PbPb}, and pp, N_{pp}, collisions the nuclear modification factor R_{AA} is defined as

$$R_{AA} \equiv \frac{L_{pp}}{\mathrm{T_{AA}N_{MB}}} \frac{N_{PbPb} \cdot \epsilon_{pp}}{N_{pp} \cdot \epsilon_{PbPb}}, \qquad (1)$$

where L_{pp} is the pp luminosity, N_{MB} represents the number of minimum bias PbPb events sampled and ϵ_{pp} and ϵ_{PbPb} are the efficiencies for reconstructing quarkonia in pp and PbPb collisions respectively.

The muon reconstruction requires that tracks in the silicon detector have matching tracks within the muon chamber. Pairs of oppositely charged muons are considered only if the χ^2 fit probability of the tracks originating from a common vertex exceeds 5% for the Υ and 1% for the J/ψs. Figure 1 shows the dimuon invariant mass for PbPb and pp data. There is a striking difference in the relative yield of the 3 states in PbPb and pp collisions. The $\Upsilon(3S)$ is almost invisible in the PbPb case.

3. Results

Figure 2 compares Υ production in PbPb and pp collisions at 2.76 TeV per nucleon pair. There is a significant suppression in PbPb with the $\Upsilon(1S)$ being the least suppressed and the $\Upsilon(3S)$ the most. The suppression of the $\Upsilon(1S)$ and $\Upsilon(2S)$ increases with centrality. One complication is that the observed $\Upsilon(nS)$ yields contain contributions from decays of heavier bottomonium states and, thus, the measured suppression is affected by the dissociation of these states.

The non-prompt contribution from b quarks to the J/ψ yield is removed via a fit of the decay length distribution of the muon pair. Figure 3 compares CMS data on prompt J/ψ production at high p_T and central rapidity to lower energy and forward rapdity results. The suppression of the high p_T J/ψ yield is stronger at higher energy. For central collisions the J/ψ yield at high p_T and $|y| \leq 2.4$ is more suppressed compared to pp collisions than low p_T J/ψ at forward rapidity.

Finally Figure 4 (Left) shows the nuclear modification factor versus N_{part} for the prompt J/ψ, $\Upsilon(1S)$ and $\Upsilon(2S)$ states. (The $\Upsilon(3S)$ is so suppressed that only an upper limit of 0.1 (95% CL) on the centrality integrated R_{AA} is reported.). The right hand panel shows centrality integrated nuclear modification factors versus the binding energy of the state.

4. Conclusions

Figure 4 shows a very characteristic pattern of suppression consistent with the sequential melting of the quarkonia states such that the largest and least tightly bound states melt at lower temperatures. The suppression of the $\Upsilon(1S)$ state is consistent with no suppression of directly produced $\Upsilon(1S)$, but rather a suppression of feed-down contribution from excited state decays only. The feed-down is expected to contribute $\approx 50\%$ at high p_T [11]. Unfortunately the uncertainties in the measurement of the feed-down contributions preclude quantitative conclusions about the suppression of directly produced $\Upsilon(1S)$.

It is of course possible that cold-nuclear-matter effects such as "nuclear absorption" could reduce the production of quarkonia in PbPb collisions [12, 13]. However modifications of the initial-state such, as shadowing of the parton distributions, are expected to have a similar effect on all the Υ states. The upcoming proton-lead run in January 2013 will be very useful in understanding the physics of cold matter. This new information should produce a clearer picture of the hot matter produced in TeV scale heavy ion collisions.

References

[1] T. Matsui, H. Satz, J/ψ Suppression by Quark-Gluon Plasma Formation, Phys.Lett. B178 (1986) 416. doi:10.1016/0370-2693(86)91404-8.

[2] A. Mocsy, Potential Models for Quarkonia, Eur.Phys.J. C61 (2009) 705–710. arXiv:0811.0337, doi:10.1140/epjc/s10052-008-0847-4.

[3] Y. Zheng, Measurements of Quarkonium Production Cross-Sections with the CMS Experiment, Nucl. Phys. B Conf. Supp.Proceedings of BEACH2012.

[4] S. Chatrchyan, et al., The CMS experiment at the CERN LHC, JINST 03 (2008) S08004. doi:10.1088/1748-0221/3/08/S08004.

[5] CMS Collaboration, Measurement of the $\psi(2S)$ meson in PbPb collisions at at $\sqrt{S_{NN}}$ = 2.76 TeV, CMS Physics Analysis Summary HIN-2012/007 (2012).
URL `http://cdsweb.cern.ch/record/1455477/files/HIN-12-007-pas.pdf`

[6] CMS Collaboration, Prompt and non-prompt J/ψ R_{AA} with 150 μb^{-1} integrated PbPb luminosity at $\sqrt{S_{NN}}$ = 2.76 TeV, CMS Physics Analysis Summary HIN-2012/014 (2012).
URL `http://cdsweb.cern.ch/record/1472735/files/HIN-12-014-pas.pdf`

[7] S. Chatrchyan, et al., Observation of sequential Upsilon suppression in PbPb collisions, accepted by Phys. Rev. Lett. (2012). arXiv:1208.2826.

[8] S. Chatrchyan, et al., Observation and studies of jet quenching in PbPb collisions at $\sqrt{s_{NN}}$ = 2.76 TeV, Phys. Rev. C 84 (2011) 024906. arXiv:1102.1957, doi:10.1103/PhysRevC.84.024906.

[9] E. d'Enterria, David G., et al., CMS physics technical design report: Addendum on high density QCD with heavy ions, J. Phys. G 34 (2007) 2307. doi:10.1088/0954-3899/34/11/008.

[10] M. L. Miller, K. Reygers, S. J. Sanders, P. Steinberg, Glauber modeling in high-energy nuclear collisions, Ann. Rev. Nucl. Part. Sci. 57 (2007) 205. arXiv:nucl-ex/0701025, doi:10.1146/annurev.nucl.57.090506.123020.

[11] T. Affolder, et al., Production of $\Upsilon(1S)$ mesons from χ_b decays in $p\bar{p}$ collisions at $\sqrt{s}$ = 1.8 TeV, Phys.Rev.Lett. 84 (2000) 2094–2099. arXiv:hep-ex/9910025, doi:10.1103/PhysRevLett.84.2094.

[12] R. Vogt, Cold nuclear matter effects on J/ψ and Υ production at energies available at the CERN Large Hadron Collider (LHC), Phys. Rev. C 81 (2010) 044903. arXiv:1003.3497, doi:10.1103/PhysRevC.81.044903.

[13] C. Lourenco, R. Vogt, H. K. Woehri, Energy dependence of J/ψ absorption in proton-nucleus collisions, JHEP 02 (2009) 014. arXiv:0901.3054, doi:10.1088/1126-6708/2009/02/014.

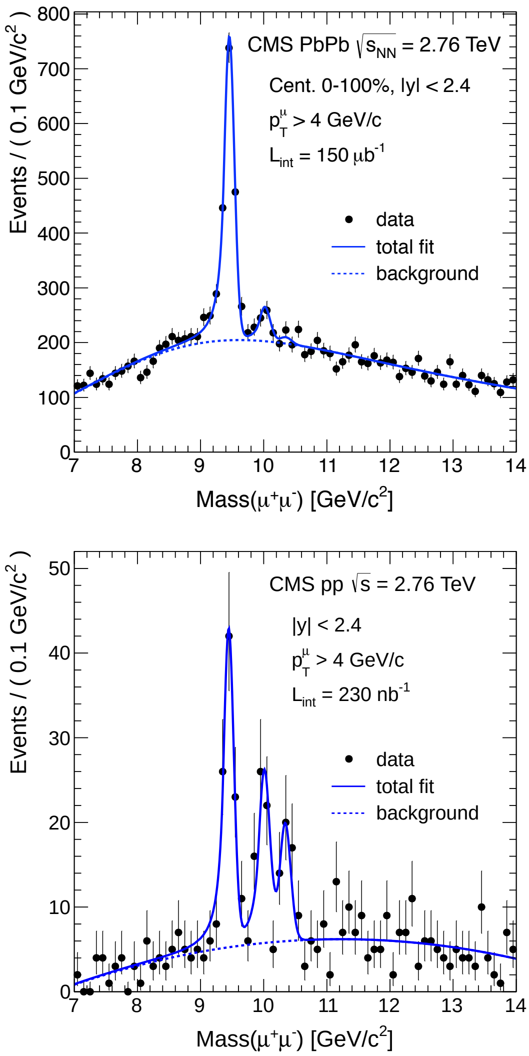

Figure 1: Dimuon invariant-mass distributions from PbPb and pp collisions at $\sqrt{s_{NN}}$ = 2.76 TeV. The same reconstruction algorithm and analysis selection are applied to both datasets, including a transverse momentum requirement on single muons of $p_T > 4$ GeV/c. The solid (signal + background) and dashed (background-only) curves show the results of the simultaneous fit to the two datasets.

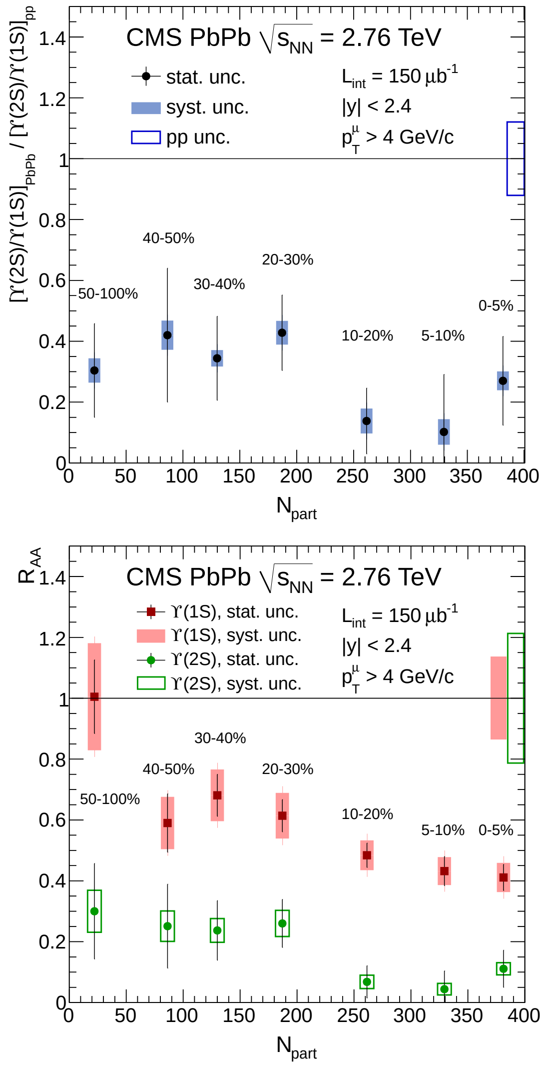

Figure 2: Centrality dependence of the double ratio (top) and of the nuclear modification factors (bottom) for the $\Upsilon(1S)$ and $\Upsilon(2S)$ states. The relative uncertainties from N_{part}-independent quantities are represented by the boxes at unity. The event centrality bins used are indicated by percentage intervals.

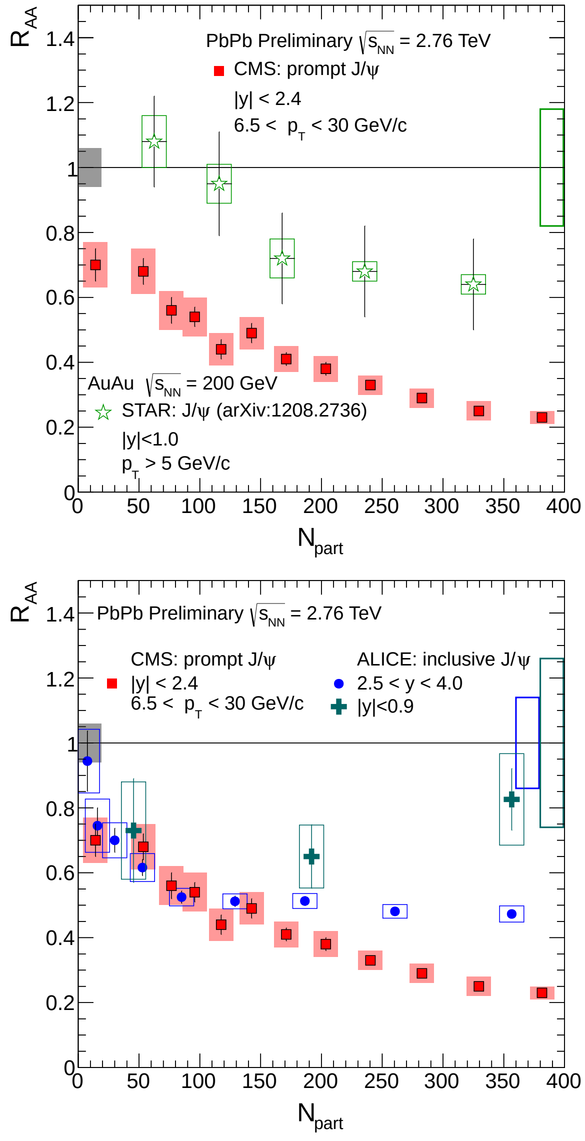

Figure 3: Nuclear modification factor versus N_{part} for prompt J/ψs. The top panel shows a comparison of CMS to lower energy data while the bottom panel compares the CMS data at central rapidity to ALICE results in the forward region.

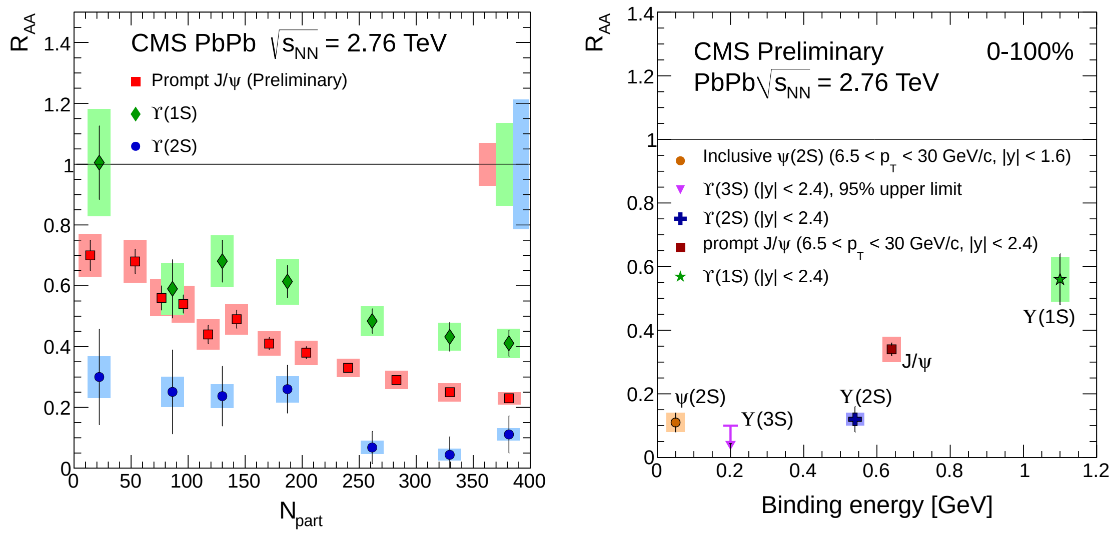

Figure 4: (Left) Nuclear modification factor versus $N_{\rm part}$ for prompt J/ψ, $\Upsilon(1S)$ and $\Upsilon(2S)$ states. (Right) Nuclear modification versus the binding energy of the state.